Molecular Crystals and Liquid Crystals Science and Technology. Section A. Molecular Crystals and Liquid Crystals

Publication details, including instructions for authors and subscription information:
http://www.tandfonline.com/loi/gmcl19

Simulation of Conoscopic Figures Using 4 × 4 Matrix Method

Toyokazu Ogasawara [a], Tomoo Akizuki [a], Yoichi Takanishi [a], Ken Ishikawa [a] & Hideo Takezoe [a]

[a] Department of Organic and Polymeric Materials, Tokyo Institute of Technology, O-okayama, Meguro-ku, Tokyo, 152-8552, Japan

Version of record first published: 24 Sep 2006

To cite this article: Toyokazu Ogasawara, Tomoo Akizuki, Yoichi Takanishi, Ken Ishikawa & Hideo Takezoe (2001): Simulation of Conoscopic Figures Using 4 × 4 Matrix Method, Molecular Crystals and Liquid Crystals Science and Technology. Section A. Molecular Crystals and Liquid Crystals, 362:1, 255-267

To link to this article: http://dx.doi.org/10.1080/10587250108025773

Mol. Cryst. Liq. Cryst., Vol. 362, pp. 255-267
Reprints available directly from the publisher
Photocopying permitted by license only

Simulation of Conoscopic Figures Using 4 × 4 Matrix Method

TOYOKAZU OGASAWARA, TOMOO AKIZUKI, YOICHI TAKANISHI, KEN ISHIKAWA and HIDEO TAKEZOE*

Department of Organic and Polymeric Materials, Tokyo Institute of Technology, O-okayama, Meguro-ku, Tokyo 152–8552, Japan

Simulation of conoscopic figures was made using 4 × 4 matrix method. After summarizing the 4 × 4 matrix method, the process for simulating conoscopic figures was briefly described. The conoscopic figures were simulated for the subphases exhibited in antiferroelectric liquid crystals, SmC^*, SmC_γ^* and SmC_A^*. The simulation was made for more complicated structures, in which SmC^* and SmC_γ^* coexist, and for a hypothetical phase, in which directors randomly distribute on smectic cones.

Keywords: simulation; conoscopic figure; 4 × 4 matrix method; antiferroelectric liquid crystal

INTRODUCTION

The orientational order in liquid crystalline (LC) phases coupled with the anisotropy of the constituent molecules gives rise to strong anisotropies in their macroscopic properties. For instance, magnetic susceptibility, refractive index and electrical conductivity are highly anisotropic in these phases. The anisotropy in refractive indices gives rise to many interesting optical effects in rich variety of structures of LC phases, which can be easily changed by external means. These optical properties are employed for applications in LC display devices. At the same time, anisotropy and its change by external fields are useful to study the molecular orientational structure in various LC phases. One of the most important techniques is optical ones, in which polarized light is often used; e.g., polarizing macroscopy, conoscopy, ellipsometry, circular dichroism, optical rotatory

* Corresponding Author.

power, Rayleigh light scattering and photon correlation spectroscopy. Among them, conoscopy is a simple but powerful technique and has been extensively used in elucidating the characteristic changes in the structures of the various subphases exhibited in the anitferroelectric liquid crystals (AFLCs) and their subphases as a function of an electric field [1–3].

The examination of a medium using a parallel beam of light between crossed polarizers reveals its optical character only along one direction. Very important additional information may be obtained by passing a strongly convergent beam of light through the medium, which enables us to examine its optical properties along many directions at the same time. The observation between crossed polarizers gives an image on a back screen due to the interference of eigen modes propagating through an anisotropic medium. This image is variously called, i.e., direction image, conoscopic figure or interference figure. The interference is of course not uniform but spatially changes, because of different path length and different birefringence depending on the path. Hence, a series of curved interference bands, which are colored in white light and bright and dark in monochromatic light, are seen. These interference bands are systematically arranged around the optic axis and are called isochromes. In addition to these isochromes there are dark brushes or isogyres, the shape of which is determined by the directional relation between the polarization of light and an index of ellipsoid.

By studying the conoscopic figures of sample cells, the following optical characteristics may be determined: (1) isotropic media may be differentiated from anisotropic ones the optic axis of which is perpendicular to a cell surface, e.g., isotropic phase and homeotropically aligned nematic LCs; (2) anisotropic media are classified optically into the uniaxial or biaxial class; (3) for uniaxial samples, the positive or negative sign of the uniaxiality of the medium is determined; (4) if the cell thickness is known, the birefringence can be estimated; (5) for biaxial samples, the direction of the optic axial plane i.e., the plane containing the two optic axes of the medium is determined; (6) the angle between the two optic axes or the optic axial angle is determined; (7) the dispersion of the optic axes may be studied. Because of these characteristics, conoscopy provides us with powerful tool to identify subphases exhibited in AFLCs.

In this article, the method of simulation of conoscopic figures using 4×4 matrix method will be described. Using the developed method, simulated conoscopic figures of subphases of AFLCs are shown. Simulation was also made for more complicated phases in which ferrielectric and ferroelectric phases coexist and for the field-induced phase-transition process to the ferroelectric state from a hypothetical phase with azimuthally random molecular orientation.

SIMULATION

4 × 4 matrix method

An appropriate formalism for describing the propagation of light in an anisotropic medium stratified along one direction is the 4 × 4 matrix method, which was introduced by Teitler and Henvis[4] and applied to liquid crystalline systems by Berreman[5]. We apply the Berreman's 4 × 4 matrix method to calculate the conoscopic figures produced by homeotropically aligned AFLC cells.

For simplicity, we assume that the medium is free of optical activity and non-magnetic i.e., μ=1. Maxwell's equations in such a medium in the absence of charges and currents (ρ=j=0) are given by

$$\nabla \times E = -\frac{1}{c}\frac{\partial H}{\partial t} \tag{1}$$

$$\nabla \times H = \frac{1}{c}\varepsilon\frac{\partial E}{\partial t} \tag{2}$$

where ε=ε(z) is the dielectric tensor, whose principal values are ε_1, ε_2 and ε_3. For a medium stratified along the z-direction, ε depends only on z. The invariance of eqs. (1) and (2) under translation of time and of x and z coordinates implies that the solutions are of the following type:

$$E = E(z)e^{i(k_x x - \omega t)} \tag{3}$$

$$H = H(z)e^{i(k_x x - \omega t)} \tag{4}$$

By substituting eqs. (3) and (4) into eqs. (1) and (2), we obtain

$$\begin{pmatrix} 0 & -d/dz & 0 \\ d/dz & 0 & -ik_x \\ 0 & ik_x & 0 \end{pmatrix} \begin{pmatrix} E_x \\ E_y \\ E_z \end{pmatrix} = i\frac{\omega}{c} \begin{pmatrix} H_x \\ H_y \\ H_z \end{pmatrix} \tag{5}$$

$$\begin{pmatrix} 0 & -d/dz & 0 \\ d/dz & 0 & -ik_x \\ 0 & ik_x & 0 \end{pmatrix} \begin{pmatrix} H_x \\ H_y \\ H_z \end{pmatrix} = -i\frac{\omega}{c} \begin{pmatrix} \varepsilon_{11} & \varepsilon_{12} & \varepsilon_{13} \\ \varepsilon_{21} & \varepsilon_{22} & \varepsilon_{23} \\ \varepsilon_{31} & \varepsilon_{32} & \varepsilon_{33} \end{pmatrix} \begin{pmatrix} E_x \\ E_y \\ E_z \end{pmatrix} \tag{6}$$

The last equation in each set does not contain derivatives with respect to z. Consequently, E_z and H_z can be expressed in terms of the other components as

$$H_z = \frac{c}{\omega}k_x E_y \tag{7}$$

$$E_z = -\frac{c}{\omega}(k_x H_y + \varepsilon_{31}E_x + \varepsilon_{32}E_y)/\varepsilon_{33} \tag{8}$$

Eliminating E_z and H_z from the other four equations, we obtain

$$\frac{d\Psi}{dz} = i\frac{\omega}{c}\Delta(z)\Psi \tag{9}$$

where

$$\Psi = \begin{pmatrix} E_x \\ H_y \\ E_y \\ H_x \end{pmatrix} \tag{10}$$

is the generalized field vector and

$$\Delta = \begin{pmatrix} -\frac{\varepsilon_{31}}{\varepsilon_{33}}\frac{c}{\omega}k_x & 1-\frac{1}{\varepsilon_{33}}\left(\frac{c}{\omega}k_x\right)^2 & -\frac{\varepsilon_{32}}{\varepsilon_{33}}\frac{c}{\omega}k_x & 0 \\ \varepsilon_{11}-\frac{\varepsilon_{13}\varepsilon_{31}}{\varepsilon_{33}} & -\frac{\varepsilon_{31}}{\varepsilon_{33}}\frac{c}{\omega}k_x & \varepsilon_{12}-\frac{\varepsilon_{13}\varepsilon_{32}}{\varepsilon_{33}} & 0 \\ 0 & 0 & 0 & -1 \\ \frac{\varepsilon_{23}\varepsilon_{31}}{\varepsilon_{33}}-\varepsilon_{21} & \frac{\varepsilon_{23}}{\varepsilon_{33}}\frac{c}{\omega}k_x & \left(\frac{c}{\omega}k_x\right)^2-\varepsilon_{22}+\frac{\varepsilon_{22}\varepsilon_{32}}{\varepsilon_{33}} & 0 \end{pmatrix} \tag{11}$$

is the 4 × 4 derivative propagation matrix of the medium. The matrix $\Delta(z)$ depends mainly on the components of dielectric tensor and therefore on the director configuration within the liquid crystal. The solution of eq. (9) can be written using a 4 × 4 transfer matrix F as

$$\Psi(z_2) = F(z_1, h)\Psi(z_1) \tag{12}$$

where h=z_2-z_1. All relevant optical parameters can be computed from F. Therefore the main problem of the 4 × 4 matrix technique is to determine the matrix F which relates the tangential component of the electric and magnetic fields at z_1 to those at z_2.

When the medium is homogeneous (i.e., Δ is independent of z over a finite distance h (=z_2-z_1) along the z-axis), eq. (9) may be integrated to give

$$\Psi(z+h) = P(h)\Psi(z) \tag{13}$$

and a closed form expression for P can always be found. An expression for P is obtained by simply expanding the exponential function in powers of the matrix Δ as

$$P = I + \frac{i\omega h}{c}\Delta + \frac{1}{2!}\left(\frac{i\omega h}{c}\right)^2\Delta^2 + \frac{1}{3!}\left(\frac{i\omega h}{c}\right)^3\Delta^3 + \cdots \tag{14}$$

where I is the 4 × 4 identity matrix.

For a medium in which the dielectric tensor depends on z, an analytic solution of eq. (9) cannot generally be found. However, a numerical solution can always be found by assuming the medium as a stack of layers of thickness h along the z-axis and the dielectric tensor ε within each layer as homogeneous. When ε varies along z, the above approximation can be made better by choosing h suffi-

ciently small. In smectic liquid crystals, the medium can be well approximated as stacks of layers along the z-axis and the method can be applied efficiently. In this way, this method is applicable to the systems with pitches shorter than the wavelength used.

With this approximation, let the matrix $P_i(h)$ denote a local propagation matrix of the i-th layer, which relates the generalized field vector Ψ of the i-th layer to that of the (i+1)-th layer. Because eq. (13) applies to each layer, we may use the equation repeatedly to obtain the transfer matrix $F(i, n)$ which relates the vectors Ψ of i-th and (i+n)-th layers as:

$$F(i,n) = P_{i+n}(h)P_{i+n-1}(h)\cdots P_{i+1}(h)P_i(h) \tag{15}$$

The transfer matrix P for each layer can be computed and the resulting P matrices are multiplied as in eq. (15) to get the final transfer matrix $F(1, N)$ for the entire N-layer system.

Then the vector Ψ_1 at the first surface is related to the vector Ψ_N at the second surface by the matrix equation

$$\Psi_N = F(1,N)\Psi_1 \tag{16}$$

The field vector at the first surface is made up of two parts with the incident and reflected wave contributions

$$\Psi_1 = \Psi_i + \Psi_r \tag{17}$$

The field at the second surface matches only a single transmitted wave field.

$$\Psi_N = \Psi_t \tag{18}$$

If the entrance and exit media are non-absorbing and isotropic, only two electric field components are needed to complete the definition of the incident wave, since the magnetic field components can be expressed in term of the electric field components in isotropic media. Therefore we write

$$\Psi_i = \begin{pmatrix} E_{ip}\cos\theta_i \\ E_{ip}n_1 \\ E_{is} \\ -E_{is}n_1\cos\theta i \end{pmatrix}, \Psi_r = \begin{pmatrix} E_{rp}\cos\theta_i \\ E_{rp}n_1 \\ E_{rs} \\ -E_{rs}n_1\cos\theta \end{pmatrix}, \Psi_t = \begin{pmatrix} E_{tp}\cos\theta_i \\ E_{tp}n_2 \\ E_{ts} \\ -E_{ts}n_2\cos\theta_t \end{pmatrix} \tag{19}$$

where (E_{tp}, E_{ts}), (E_{rp}, E_{rs}) and (E_{ip}, E_{is}) are the p- and s-polarized electric components of the transmitted (t), reflected (r) and incident (i) waves, respectively. n_1 and n_2 are the refractive indices of the entrance and exit media, respectively. θ_i is the incidence angle and θ_t is defined by Snell's low

$$n_1\sin\theta_i = n_2\sin\theta_t \tag{20}$$

By substituting eqs. (17), (18) and (19) in eq. (16), we obtain four linear equations for E_{tp}, E_{ts}, E_{rp} and E_{rs}. Therefore, the transmitted electric components can

be obtained by solving these linear equations. The description of this general case can be found in the original treatment by Berreman[5].

Simulation of conoscopic figures

We now apply the Berreman's 4 × 4 matrix method to simulate the conoscopic figures exhibited by homeotropically aligned AFLC cells. It is assumed that crossed polarizers give complete dark for normally incident light and an objective lens system is free from spherical and other aberrations for a monochromatic light used. Figure 1 shows the experimental geometry and the coordinate system used in the conoscopic calculations. A collimated light beam passing through a polarizer making at an angle of $\pi/4$ with respect to the x-axis is focused onto homeotropically aligned AFLC cells by an objective lens. The transmitted beam from the sample cell then passes through a crossed analyzer to form conoscopic figures.

For simplicity we assume that each ray of the convergent beam from the objective lens can be represented as a plane wave. By the incidence of an electric field, E_{ix} and E_{iy}, after passing through the polarizer, p- and s-polarized components of the convergent beam can be written as

$$\begin{pmatrix} E_{ip}\cos\theta_i \\ E_{is} \end{pmatrix} = \begin{pmatrix} \cos\alpha & \sin\alpha\cos\theta_i \\ -\sin\alpha_i & \cos\alpha\cos\theta_i \end{pmatrix} \begin{pmatrix} E_{ix} \\ E_{iy} \end{pmatrix} \tag{21}$$

Here, α, β, γ and θ_i are angles defined as

$$\alpha = Tan^{-1}\left(\frac{x}{y}\right) \tag{22}$$

$$\theta_i = Tan^{-1}\left(\frac{\sqrt{x^2+y^2}}{L}\right) \tag{23}$$

where (x, y) are a point on a screen. L is the distance between the sample and a screen. Similarly, by p- and s-polarized components of a transmitted divergent beam, transmitted electric field components E_{tx} and E_{ty} can be written as

$$\begin{pmatrix} E_{tx} \\ E_{ty} \end{pmatrix} = \begin{pmatrix} \cos\alpha & -\sin\alpha \\ \sin\alpha & \cos\alpha \end{pmatrix} \begin{pmatrix} E_{tp}\cos\theta_t \\ E_{ts} \end{pmatrix} \tag{24}$$

Using eqs. (16) ~ (21) and (24), we can obtain electric fields of transmitted light at (x, y) and simulate transmittance for conoscopic figures.

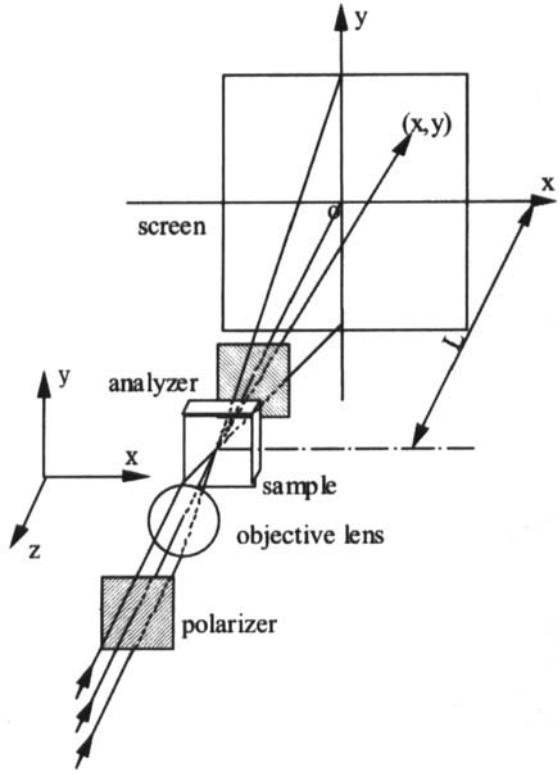

FIGURE 1 Experimental geometry and coordinate system used in the conoscopic calculation

EXPERIMENTAL AND SIMULATED RESULTS

Experimental results

Figure 2 shows typical conoscopic figures observed in various phases in a homeotropically aligned AFLC cell of MHPOBC[1]. The index ellipsoids are also illustrated. All the tilted phases in the absence of a field give rise to a conoscopic figure almost the same as that of a untilted phase. Namely the conoscopic figures in these cases consist of a Maltese cross with the isogyres parallel to the crossed polarizers and a series of concentric circular isochromes. This is because all the tilted phases have helical structures giving rise to a macroscopic uniaxial medium with optic axis parallel to the layer normal in the absence of a field.

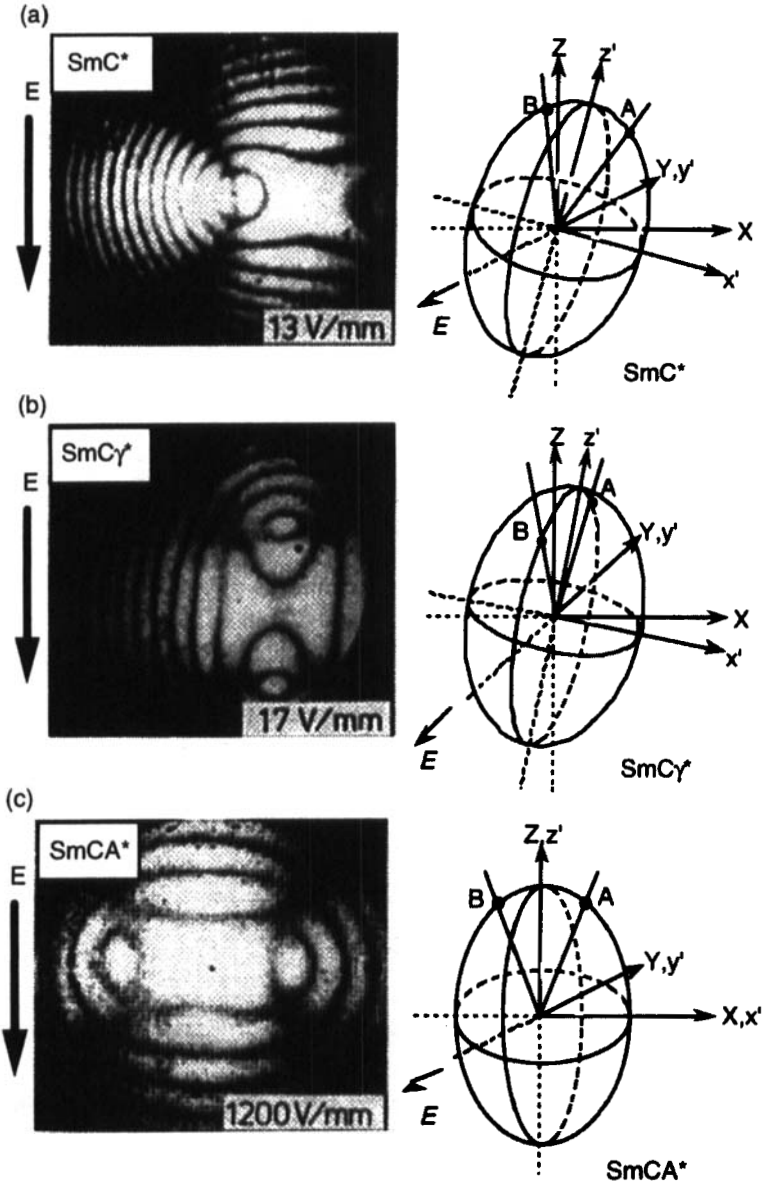

FIGURE 2 Conoscopic figures and their index elli psoids in the SmC*, SmC_γ* and SmC_A* phases

In the SmC* phase, the uniaxial profile due to the helical structure in the absence of a field changes to a biaxial one upon the application of a field. This is because of the field-induced helix unwinding and the weak biaxiality of the tilted

SmC^* layers. The center of the conoscopic figure shifts along the direction perpendicular to the field. This means that the acute bisectrix in the medium is at an angle with respect to the layer normal. The splitting direction of the isogyre indicates that the optic axial plane containing two optic axes of the resulting biaxial medium is perpendicular to the field. Namely the refractive index for the polarization direction perpendicular to the tilt plane is larger than that for the parallel polarization. The biaxiality originates from the hindered rotation of molecule along its long axis. All the conoscopic figures so far reported have the same anisotropy as the present case. The directional sense of the shift of the center specifies the sign of the spontaneous polarization.

The field dependence of the conoscopic figures in the ferrielectric SmC_γ^* phase is somewhat complicated. The uniaxial figure in the absence of a field changes to a biaxial one upon the application of a field with the shift of the center in the same direction as in the SmC^* phase. But unlike in the SmC^* phase, the optic axial plane in this phase is parallel to the field at low fields (Fig. 2(b)), and switches to the perpendicular direction associated with the field-induced further transition to SmC^* at higher fields.

The field-induced changes in the conoscopic figures of the antiferroelectric SmC_A^* phase are also quite characteristic of this phase. A uniaxial figure changes to a biaxial one with the optic axial plane perpendicular to the field under increasing a field strength. However, there is no significant shift of the center up to the maximum field strength of 1200 V/mm used in the experiment[1].

Simulated results

Figure 3 shows the simulated conoscopic figures and molecular orientational structures corresponding to the field induced structures predicted by Ising model in various phases. For the calculations, ε_1=2.250, ε_2=2.259, ε_3=2.690, the tilt angle θ=17°, wave length of incident wave λ=632.8 nm and refractive indices of entrance and exit media n_1=n_2=1.0 were used. Typical conoscopic figures can be simulated well by the Ising structures in each phase.

In order to show the applicability of this simulation method, the conoscopic figures for more complicated structures were simulated. They are (1) the phase consisting of ferroelectric and ferrielectric phases[6] and (2) a hypothetical SmC_R^* phase, in which the director distribution in azimuthal angle is random[7]. These phases were proposed but not yet confirmed.

Recently, Panarin *et al.*[6] proposed the coexistence of two different subphases (ferroelectric and ferrielectric phases) to explain the unusual conoscopic figure which shows four centers. Figure 4 illustrates the system for the calculation. We

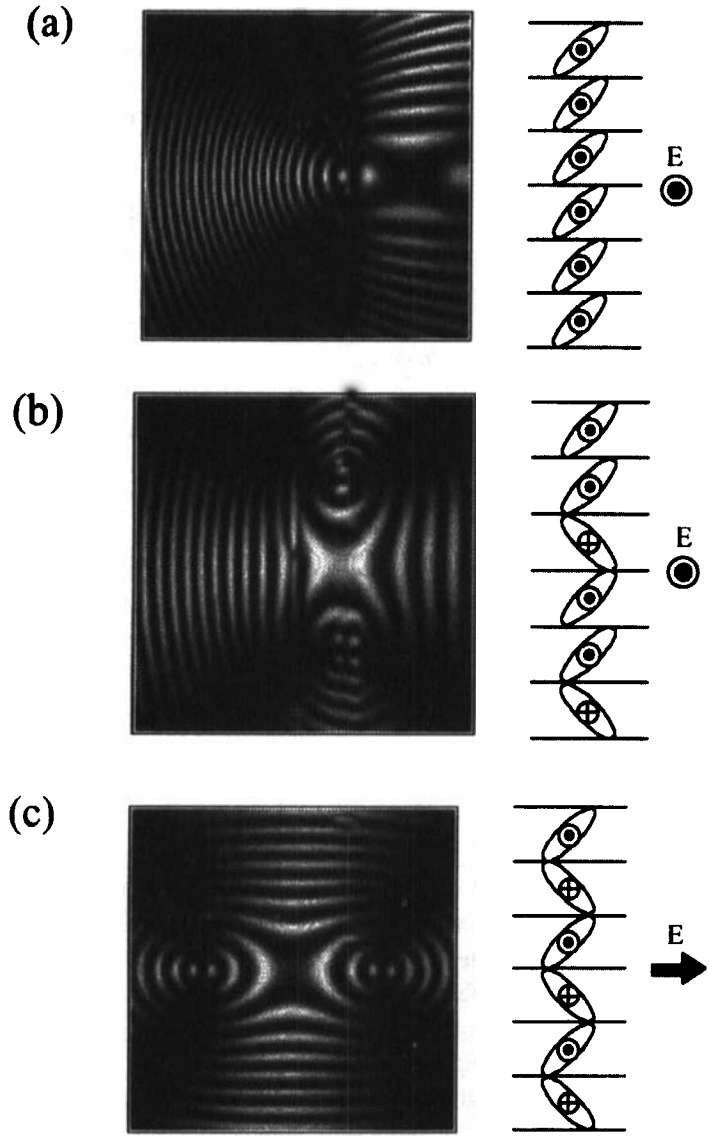

FIGURE 3 Simulated conoscopic figures in the (a) SmC^*, (b) SmC_γ^* and (c) SmC_A^* phases using the molecular orientational structures based on the Ising model

used 200 μm cell, in which L is a thickness of ferroelectric region and the rest is the ferrielectric region. As the ferrielectic phase, the SmC_γ^* phase was used. The

parameters used in the calculation were as follows: a dielectric constant along the molecular long axis ε_1=2.690, one along the spontaneous polarization ε_2=2.259 and one perpendicular to these axes ε_3=2.250, a tilt angle θ=18°, a layer spacing d=4 nm. The cell was sliced into 50000 slabs along the substrate normal for the calculation.

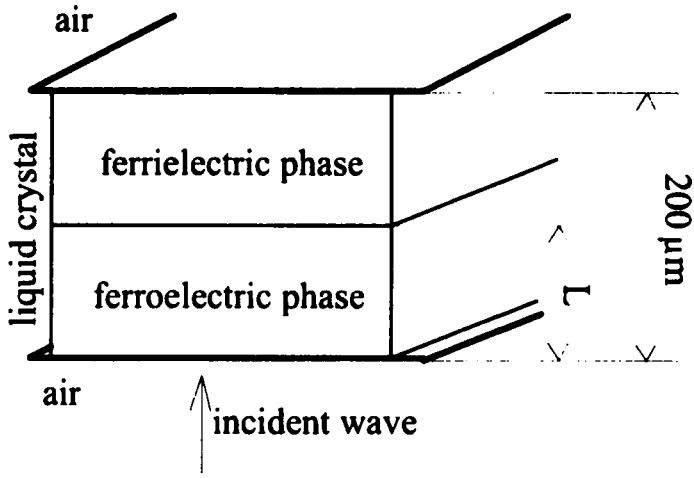

FIGURE 4 The system for the simulation of conoscopic figure for a hypothetical structure consisting of SmC*(thickness L) and SmC_γ^*

Figure 5 shows simulated conoscopic figures for cells with various L; (a) L=150 μm, (b) L=100 μm and (c) L=50 μm. In all the figures, the isogyres of the conoscopic figures shift along the direction perpendicular to an electric field. However, the isogyres are blurred and give complicated structures depending on L. It is difficult to observe four centers, as suggested by Panarin *et al.*[6], in the present structures.

Let us next show the conoscopic figures simulated for the field-induced phase transition process from the azimuthally random phase to the ferroelectric state. The existence of this phase was proposed to interpret the mechanism of so-called V-shaped switching[7], but has not been confirmed and was rather denied[8]. Simulation was also made for field-induced helix unwinding process in the SmC* phase to compare with that in the random phase. In this calculation, we used the same parameters as those used in the previous simulation.

Figure 6 shows two series of simulated conoscopic figures under three electric field strengths in the SmC* phase (upper column) and the random phase (lower

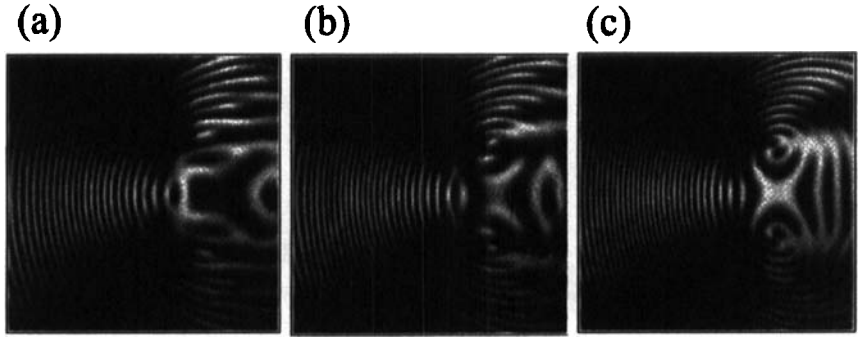

FIGURE 5 Simulated conoscopic figures for cells of 200 μm thickness, in which ferroelectric and ferrielectric structures coexist. The thickness L for the ferroelectric region are (a) L=150 μm, (b) L=100 μm and (c) L=50 μm

column). In both phases, the conoscopic figure shows uniaxial figures due to a helical structure (SmC^*) and a random orientation (SmC_R^*) in the absence of an electric field. In the SmC^* phase, the unwinding of helix was simulated by determining the deformation of helix under the influence of dipolar interaction between the spontaneous polarization and an electric field and the assumption that the pitch does not change, in other words one point for every one pitch is pinned. As shown in Fig. 6 (upper column), the isogyre of conoscopic figure shifts along the direction perpendicular to the field but do not split, maintaining the uniaxial profile at low fields. This behavior was actually observed in a ultrashort pitch compound[9]. Then, it changes to a biaxial one when the helix is almost unwound upon the application of a very high field. In the azimuthally random phase, unlike the SmC^*phase, the isogyre of conoscopic figure shifts and the uniaxial profile changes to a biaxial one even at very low fields. This is because of the azimuthal distribution change on smectic cones by the field-induced reorientation of molecules. These results indicate that the random phase can be distinguished from the conventional SmC^* phase by means of conoscopy.

CONCLUSION

Conoscopic figures for various known phases were simulated using 4 × 4 matrix method. The simulation was also made for some hypothetical phases, and suggested the usefulness to identify complicated phase structures.

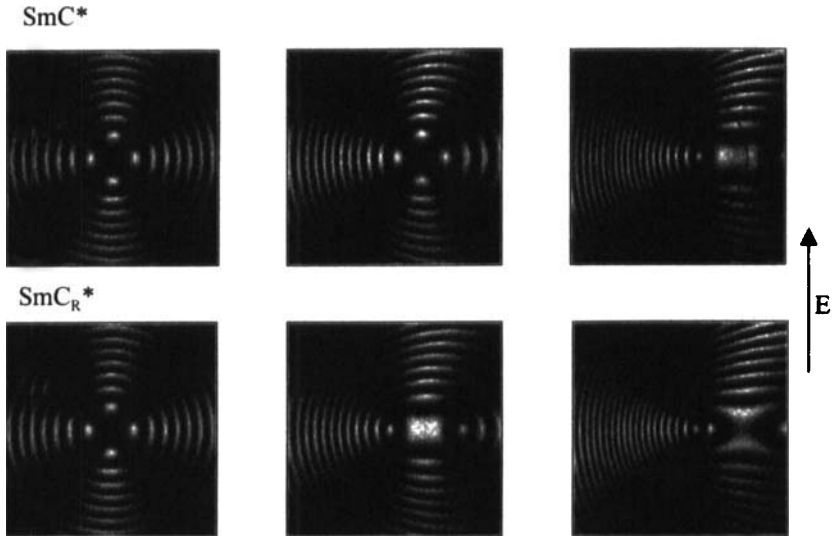

FIGURE 6 Simulated conoscopic figures under three electric field strengths in the SmC* phase (upper column) and the random phase (lower column)

References

[1] E. Gorecka, A. D. L. Chandani, Y. Ouchi, H. Takezoe and A. Fukuda, *Jpn. J. Appl. Phys.*, **29**, 131 (1990).
[2] T. Fujikawa, K. Hiraoka, T. Isozaki, K. Kajikawa, H. Takezoe and A. Fukuda, *Jpn. J. Appl. Phys.*, **32**, 985 (1993).
[3] T. Akizuki, K. Miyachi, Y. Takanishi, K. Ishikawa, H. Takezoe and A. Fukuda, *Jpn. J. Appl. Phys.*, **38**, 4832 (1999).
[4] S. Teitler and B.W. Henvis, *J. Opt. Soc. Am.*, **60**, 830 (1970).
[5] D. W. Berreman, *J. Opt. Soc. Am.*, **62**, 502 (1972).
[6] Yu. P. Panarin, O. Kalinovskaya, J. K. Vij and J. W. Goodby, *Phys. Rev. E*, **55**, 4345 (1997).
[7] S. Inui, N. Iimura, T. Suzuki, H. Iwane, K. Miyachi, Y. Takanishi and A. Fukuda, *J. Mater. Chem.*, **6**, 71 (1996).
[8] B. Park, S. S. Seomun, M. Nakata, M. Takahashi, Y. Takanishi, K. Ishikawa and H. Takezoe, *Jpn. J. Appl. Phys.*, **38**, 1474 (1999).
[9] K. Itoh, Y. Takanishi, J. Yokoyama, K. Ishikawa, H. Takezoe and A. Fukuda, *Jpn. J. Appl. Phys.*, **36**, L784 (1997).